Additive Manufacturing 75 (2023) 103754

Contents lists available at ScienceDirect

Additive Manufacturing

journal homepage: www.elsevier.com/locate/addma

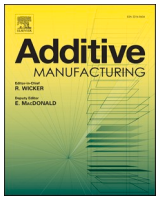

X-Ray Computed Tomography performance in metrological evaluation and characterisation of polymeric additive manufactured surfaces

Daniel Gallardo [a,*], Lucía-Candela Díaz [a], Roberto Jiménez [b], Marta Torralba [b], José Antonio Albajez [a], José Antonio Yagüe Fabra [a]

[a] I3A, Universidad de Zaragoza, María de Luna 3, 50018 Zaragoza, Spain
[b] Centro Universitario de la Defensa, A.G.M., Carretera Huesca s/n, 50090 Zaragoza, Spain

ARTICLE INFO

Keywords:
Polymeric additive manufacturing
X-ray computed tomography
Surface characterisation

ABSTRACT

Surface characterisation has always been an important aspect in quality control for industrial parts. With the development of additive manufacturing (AM) technologies and the design freedom they provide, new measuring techniques have become necessary for inspection of inner elements and hidden surfaces. X-ray computed tomography (XCT) has the potential for this purpose. Its performance in surface characterisation has been studied mainly for new metallic AM technologies due to its extended use in industrial products; however, it is not possible to directly extend this knowledge to polymeric AM surface characterisation, due to the material, manufacturing process itself and behaviour with X-rays. In this paper, a study of different polymeric AM surfaces by means of XCT is presented, taking into consideration the layer-by-layer technology and geometrical parameters (angle of inclination, layer thickness). Areal and linear roughness parameters are extracted to create a comparison between XCT measurements and reference measurements with a calibrated focal variation microscope (FVM). A reasonably achievable geometrical magnification for a polymeric AM assembly with industrial part dimensions (28 μm voxel size for a 50 mm × 55 mm × 60 mm object) is demonstrated to be suitable for roughness evaluation with an acceptable precision. Results show that it is possible to evaluate roughness in FDM and Polyjet technologies with linear parameters, while areal parameters are more suitable for SLS parts; also, post process has an important role in surface characterisation, but its effect is different depending on the technology.

1. Introduction

In recent years, quality control of industrial parts has reached a new level of possibilities due to a new evaluation technology: X-ray computed tomography (XCT) [1–4]. This technique is based on the acquisition of 2D X-ray images of the evaluated part to reconstruct a 3D model of the object. Its main advantage is its ability to characterise not only the external surface of the part, but also the internal elements; thus, a non-destructive evaluation of a mechanical assembly can be done [5].

XCT has been used for years for medical purposes [6]; however, its application for industrial quality control is relatively new. As a result, the standardization of the calibration procedures for XCT devices is still in development [1,7]. Studies have been conducted on the design of parts which could be calibrated and serve as reference standards for the uncertainty estimation according to normative [8–10].

Several studies have also investigated the most optimal conditions for XCT measurements [11,12], and different methods to correct aspects that could create defects in the final reconstruction, such as beam hardening [13–15].

One of the main causes of the increasing interest in XCT in the latest years is the metrological requirements in terms of industrial part evaluation [3,16]. This is mostly due to the evolution of additive manufacturing (AM) [17–23], which allows the producers to create more complex and sophisticated designs [21,24–26] with lower material usage, even including internal geometries or freeform surfaces which are not possible to measure with traditional metrological devices.

AM was used at first as a technology to produce prototypes in early design stages, with only formal characteristics, due to its limitations. However, the development of new AM technologies, with improved mechanical and thermal characteristics, and the usage of high-quality materials, have allowed to manufacture end-use products with similar performances as the ones made by traditional manufacturing techniques

* Corresponding author.
E-mail address: dgallardo@unizar.es (D. Gallardo).

https://doi.org/10.1016/j.addma.2023.103754
Received 21 February 2023; Received in revised form 13 July 2023; Accepted 22 August 2023
Available online 26 August 2023

(such as machining, turning, etc.).

Among the additive manufactured materials, metals have been widely investigated, also for XCT research due to their stability [27,28]. In this aspect, the lack of dimensional stability of polymers makes these materials less suitable than metals for reference parts; however, they have a great interest in industry due to their versatility and their widespread usage in some industrial applications [29,30].

Regarding quality control, one of the most important fields of study for industrial parts is the dimensional accuracy. This, in terms of metrology, is normally attached to macro geometries and their dimensions as diameters, form errors, distances between elements, etc. However, the control and evaluation of surface topography and roughness results is critical for the functionality of certain parts. This becomes even more important for objects manufactured by AM because they have a natural higher surface roughness, mainly due to its layer-by-layer technology. Regarding this field, several studies have been made to evaluate roughness of metal and polymeric additive manufactured surfaces, relying on the normative which defines specifically the process for its characterisation [31–35].

The issue with AM surface characterisation is the difficulty of a generalisation among the technologies, materials, etc., because each technology produces a different topography, even from one print to other. Efforts have been made to create predictive models for certain technologies [36–38].

In case of XCT evaluation, material takes a higher importance due to the effect of material density and thickness in X-ray penetration [39]. This effect is more present in micro geometries (as surface roughness) because their size is closer to the voxel size, hence, being more sensible to any parameter modification. Metallic AM surfaces have already been studied previously by XCT [40].

With all of this information in mind, the study registered in this paper is focused on the surface characterisation of different polymeric AM features by means of XCT. A range of roughness profiles with predicted average roughness Ra following predictive models [37,38] have been designed, taking into consideration relevant parameters as layer thickness and angle of inclination.

The main objective is to evaluate the performance of XCT when measuring these features, so reference measurements have been taken by traditional metrological devices to compare to XCT results. Also, XCT measurement settings have been tested to check their influence in surface characterisation. In this case, the most relevant parameter has been geometrical magnification, so three voxel sizes have been selected to amplify the range of the study.

Because the aim is to create a study as complete as possible, three polymeric AM technologies with different manufacturing principles have been used to create the evaluated features: Fused Deposition Modelling (FDM), Selective Laser Sintering (SLS) and Polyjet. The manufacturing process itself is another parameter that is able to create different surface topography even with similar materials.

2. State of the art

The characterisation of the surface topography of industrial parts, as indicated before, is an interesting parameter to take into consideration for manufacturers, and it has been a field of study recently for many research groups.

In terms of metrology, roughness measurements generally can be divided into linear parameters, extracted from profiles along the surface, and areal parameters, obtained from small areas of the surface. Both characteristics and the process followed for its calculations are ruled by specific normative [31,32,35] which is applied in this paper. Also, digital filtering of surfaces and profiles has been studied [41] for its application to extract roughness parameters.

Normative made for surface texture measurement is typically followed by studies performed for XCT evaluation [42], although it is not specifical for this technology. Surfaces are converted to.STL files and post processed in roughness measurement software. Not only the traceability of measurements made by XCT is studied [40], but also factors affecting the performance of this technology, as the filter used [43], the surface determination [44], or whether the surface characterised is an external or internal feature. Also, unique AM features as re-entries are investigated [45] in order to optimise and adapt the roughness parameters to these characteristics. As the surface roughness has an importance into form and functionality of parts, also its influence on XCT dimensional measurements is studied elsewhere [46].

The surface texture of the most used polymeric AM technologies has been also investigated: for SLS [47], FDM and Polyjet parts [48], even building predictive models [37,38] based on two relevant parameters (angle of inclination and layer thickness). For this purpose, high precision devices have been used, as focal variation, confocal and optical microscopes, and tactile profilometers.

For surface texture evaluation, simple parts with small geometries, typically planes, are designed. The objective is to have enough surface area to obtain the roughness parameters according to normative; in designed parts for XCT studies, reducing the size of the test object helps achieving a better geometrical magnification and, thus, a smaller voxel size.

In the following table, a brief summary of some objects of study designed specifically for surface evaluation by XCT is presented. Table 1.

All objects of study summarized are manufactured in high performance metal alloys, some of them produced by AM [40,49] due to the focus of their studies on these technologies. All surfaces evaluated in the four objects of study selected are planes. The dimensions of the objects vary from a similar size as the evaluated area (5 mm × 5 mm × 5 mm in [49]) to a bigger part with different zones (15 mm × 15 mm × 30 mm in [40]). Generally, areal surface evaluation is chosen over linear profiles, unless in [40], with different area sizes, but always square-shaped as indicated in normative [33].

3. Methodology

In this section, the theoretical models followed to estimate the average roughness, the design of the object of study and the process followed for the evaluation of the geometries is presented.

3.1. Theoretical models

A first predictive model [37] (Ahn model) is used as a reference for the design of the object of study. Its aim is to estimate the theoretical average roughness (Ra') created by inclined ramps on AM parts; the calculations are based on Eq. 1:

$$Ra' = \frac{1000t}{2}\left|\frac{\cos((90-\theta)-Ø)}{\cos Ø}\right| \quad (1)$$

Where t is the layer thickness, θ is the angle of inclination of the ramp (from the vertical), and Ø is the angle deviation of the vertical walls. Considering $Ø = 0$ for a theoretical and, thus, ideal scenario, the two main parameters are layer thickness and angle of inclination. With this theoretical knowledge, the aim of this experiment has been to create a

Table 1
Summary of surface evaluation objects of study.

Research group	Material	Evaluated surface dimensions
National Physics Laboratory (UK)[40]	Ti64 alloy	14 mm profiles
University of Huddersfield (UK) [42]	Ti6Al4V ELI	8 × 8 mm area
Tusas Engine Industries (Turkey)[49]	Inconel 718, Ti6Al4V	4.2 × 4.2 mm area
University of Huddersfield (UK) [50]	Ti6Al4V	5 × 5 mm area

range of surfaces with smoother (lower Ra') and rougher (higher Ra') features, using the layer-by-layer AM technology. Principle can be seen in Fig. 1.

A second theoretical predictive model [38] is used for FDM parts. Its aim is to create a more realistic model in terms of geometry, taking into consideration the roundness of the deposited filaments. In Fig. 2, a cross-section of two deposited filaments is displayed. Vertical red line in the merge of the filaments is included to avoid profiles with negative draft angle.

Calculated area is shown in Fig. 3; horizontal line height is calculated for each profile in order to obtain the same area (in grey) above and below it.

Calculations of theoretical average roughness (Ra') are made following Eq. 2:

$$Ra' = \frac{1}{L} \int_0^L |f(x)|dx \quad (2)$$

Where L is the horizontal measurement length, and f(x) is the function that defines the roughness profile.

3.2. Artefact design and geometries evaluated

A preliminary experiment was conducted with a wide range of evaluated geometries. Several individual parts were manufactured including ramps with four different inclinations from 30º to 75º, (increase of 15º between ramps). Two design typologies were created: two-faced parts, which include two ramps (30º-60º and 45º-75º) and four-faced ramps, including the four inclinations. Two-faced parts design is intended to be easier to include in an assembly, while four-faced parts design has the main objective of joining as many measurands possible in only one part. Complementary angled ramps were designed in the lower face to ease the fixture in the measurement device, allowing to place each measured ramp in an approximate perpendicular position with the optical measuring device lens. 3 AM technologies were used for the production of the parts: fused deposition modelling (FDM), Polyjet and selective laser sintering (SLS). Polyjet is an AM technology, similar to multi jetting, which is based on the technology of traditional 2D ink jetting devices. Instead of ink, the material used by the Polyjet machine is a photopolymerised resin which is cured by UV lights. As other AM technologies, building of the parts is done layer-by-layer. Materials used are PLA for FDM parts, photopolymerisable resin Rigur RGD450 for Polyjet, and nylon PA12 for SLS.

Parts are printed in two layer-thickness values: 0.1 mm and 0.2 mm. As Polyjet technology nominal layer thicknesses are below these values (16–48 μm), simulated layer thicknesses of 0.096 mm and 0.192 mm (multiples of the nominal layer thickness) are made in order to approach

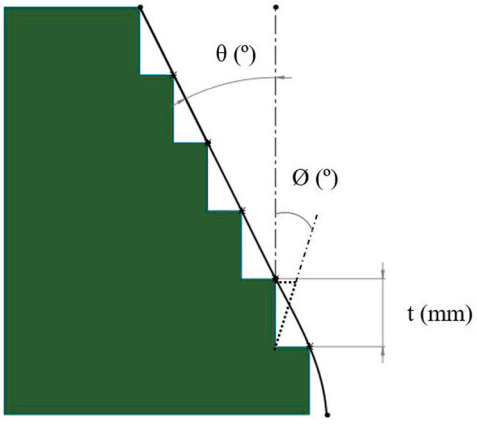

Fig. 1. Layer-by-layer AM principle and roughness prediction in Ahn model [37].

Fig. 2. Cross-section of 2 filaments (based on [38]).

it to the other technologies' layer thicknesses and, thus, to have a more comparable geometries in the study. Three copies of each part have been manufactured to amplify the range of available parts; the parts with fewer defects are selected to obtain a comparable study since severe defects could affect randomly the roughness data obtained.

General dimensions of the two-faced parts are displayed in Fig. 4, and general dimensions of the four-faced parts are displayed in Fig. 5. Parts are designed to obtain an evaluable length in upper faces of at least 15 mm for profiles and 5 × 5 mm for areas.

Post process on the parts has been only necessary for Polyjet and SLS parts. They have been cleaned by pressurized water for Polyjet parts and compressed air for SLS. Post process was necessary to remove the outer layer of support material remaining in Polyjet parts, which is a result of the process itself, and pressurized water is the method recommended by the manufacturer. In the case of SLS, the aim is to reduce the amount of unfused powder remaining in the surface, without damaging the stepped stairs – abrasive powder is possible to be added to the compressed air; it would clean the surface deeper but also would erode the steps.

Preliminary experiment measurements were proceeded by the reference device, a focal variation microscope (FVM) InfiniteFocusSL of Alicona, to select the most adequate features for future XCT evaluation. As one of the objectives is to create an object of study as compact as possible, one part was selected for each AM technology. Second criteria used for the selection was the comparison between average roughness deviation (Ra) measured in FVM and theoretical average roughness (Ra') based on the predictive models [37,38] as explained in Section 3.1.

An ad hoc assembly with the selected parts is designed in order to optimise the surface evaluation by means of XCT and the reference device. The main objective of the design is to ease the orientation of the part for the reference measurements, as done for the preliminary experiment, being able to fit every surface to be measured in a horizontal plane, thus, incorporating complementary-angled ramps in the opposite side of the part. Also, for the XCT measurements, the aim has been to make the design as much compact as possible, to improve the geometrical magnification. As the part is composed by components manufactured by different AM technologies, a polymeric FDM base to support those components is created. Additional ramps, similar to those present in individual parts, were added into the base to amplify the range of geometries evaluated. The result is an assembly with general dimensions 50 mm × 55 mm × 60 mm, shown in Fig. 6. Sinusoidal profiles present in the assembly are intended for future experiments and, thus, their results were not included in this paper.

As a result, geometries evaluated in the experiment studied in this paper are listed in Table 2. All geometries indicated are inclined ramps, as mentioned before.

3.3. Measurement procedure

Three XCT measurements were taken for the whole assembly with a Zeiss Metrotom 1500/225 kV, with three different voxel sizes (28, 54 and 75 μm), following this procedure:

- 28 μm is the smallest voxel size allowing the study area to be scanned in a single tomography.
- A voxel size of 54 μm is obtained under similar magnification conditions but applying a 2x binning. The binning process combines the information of several voxels (four voxels in 2x binning) to generate

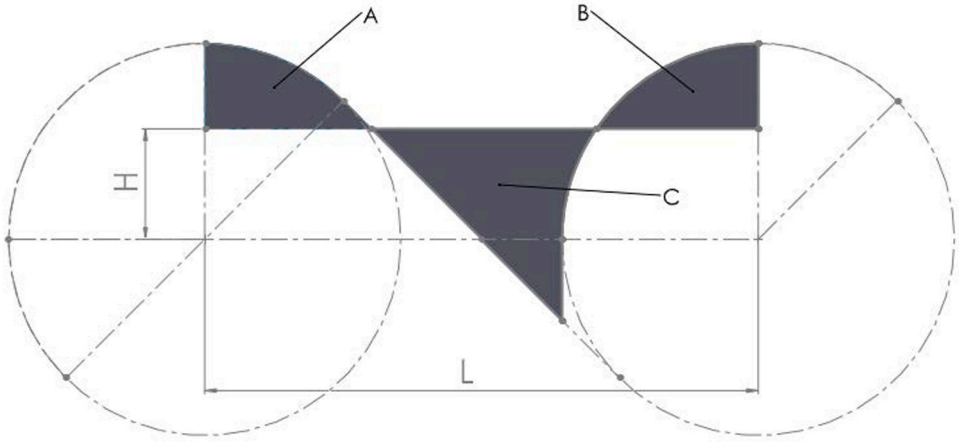

Fig. 3. Example of areas (in grey) used for theoretical Ra calculation (based on [38]).

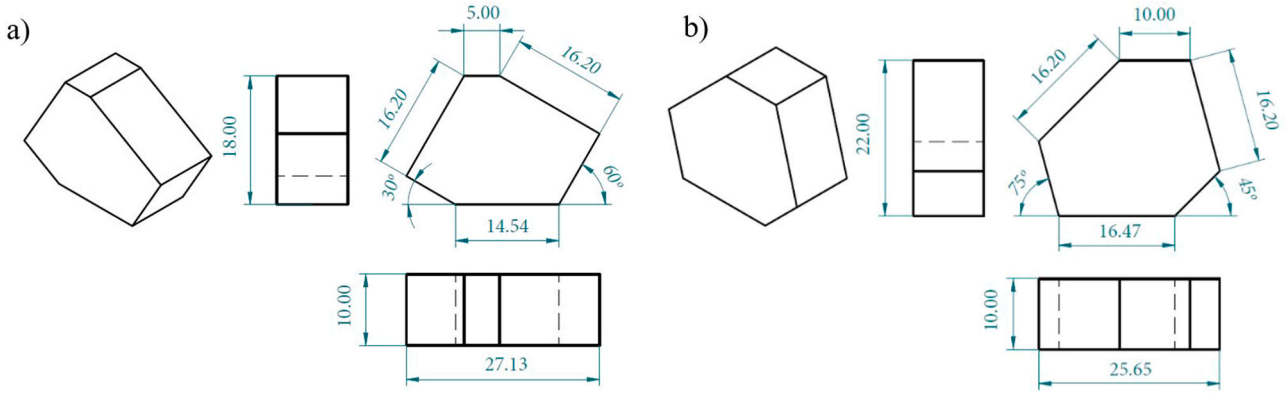

Fig. 4. Nominal dimensions (in mm) of two-faced parts. Manufactured by FDM and Polyjet. a) 30º - 60º b) 45º - 75º.

a single voxel, reducing the size of the generated files and accelerating the tomography analysis process.
- 75 μm has been obtained increasing the source-to-object distance and thus, reducing the magnification. 2x binning process is also utilised for this tomography.

Settings selected for the measurements are listed in Table 3.

A physical filter of aluminium with 2 mm of thickness was used for all the measurement to obtain a better contrast possible between polymer and background (air), and to ensure the correct penetration of all the geometries, since some areas could be too thick. Tomographies were processed in the software VGStudio Max 3.4.2, with a preliminary general surface determination in Advanced mode, and local gradient surface determination for each geometry after ROI definition, with a 4-voxel search distance. For both general and local surface determinations, default ISO50 method was used in the software. A mesh for each element was exported in.STL format, using the "manual" point reduction to set the tolerance in the minimum achievable (1/1000 voxel size), in Ray-based mode. Reconstruction of the complete volume and an example of an individual.STL ramp is shown in Fig. 7. 28 μm voxel size tomography has been made with no-binning process into the detector, while 54 μm and 75 μm tomographies have been made with a 2 × 2 binning. As a consequence, for 28 μm XCT a higher number of projections were necessary to achieve this resolution.

Prior to XCT evaluation, as mentioned previously, reference measurements were taken by a FVM InfiniteFocusSL of Alicona; a 10x magnification lens was used, lateral resolution of 8 μm and vertical resolution of 130 nm. The complete features were scanned and a.STL file was exported for each geometry. Three profiles of 15 mm length and three areas of 4 × 4 mm, equally distributed along the surface, are extracted from each geometry for roughness evaluation.

Areal and linear roughness parameters were calculated with metrological software Gwyddion 2.60.

Three surface characteristics of each feature are intended to be evaluated, both for linear profiles and areas:

- Average roughness parameters (Ra, Rq, Sa, Sq)
- Maximum and minimum values of peaks and valleys (Rz, Rp, Rv, Sz, Sp, Sv).
- Form and material distribution (Rsk, Rku, Ssk, Sku).

Average roughness parameters are divided into arithmetical average roughness (Ra, Sa), which are calculated by the mean value of the feature, and quadratic average roughness (Rq, Sq), which are calculated with the quadratic mean value.

Maximum roughness parameters consider the mean of several maximum values according to normative: 5 higher peaks (Rp, Sp), 5 lower valleys (Rv, Sv) and both (Rz, Sz). Therefore, Rz and Sz is a combination of Rv and Rp, and Sv and Sp, consecutively.

Skewness (Rsk, Ssk) and kurtosis (Rku, Sku) represent the form and material distribution of the feature. Skewness is related to the symmetry of the profile around the median lane; positive skewness indicates the presence of higher peaks, while negative skewness means deeper valleys. Kurtosis evaluates the sharpness of the profile; values of Rku, Sku > 3 are related to sharper peaks and valleys while values < 3 indicate flatter and rounder profiles.

Parameters were selected according to ISO 21920–3:2021 [35] for linear profile evaluation and to UNE-EN ISO 25178–2 [32] for areal

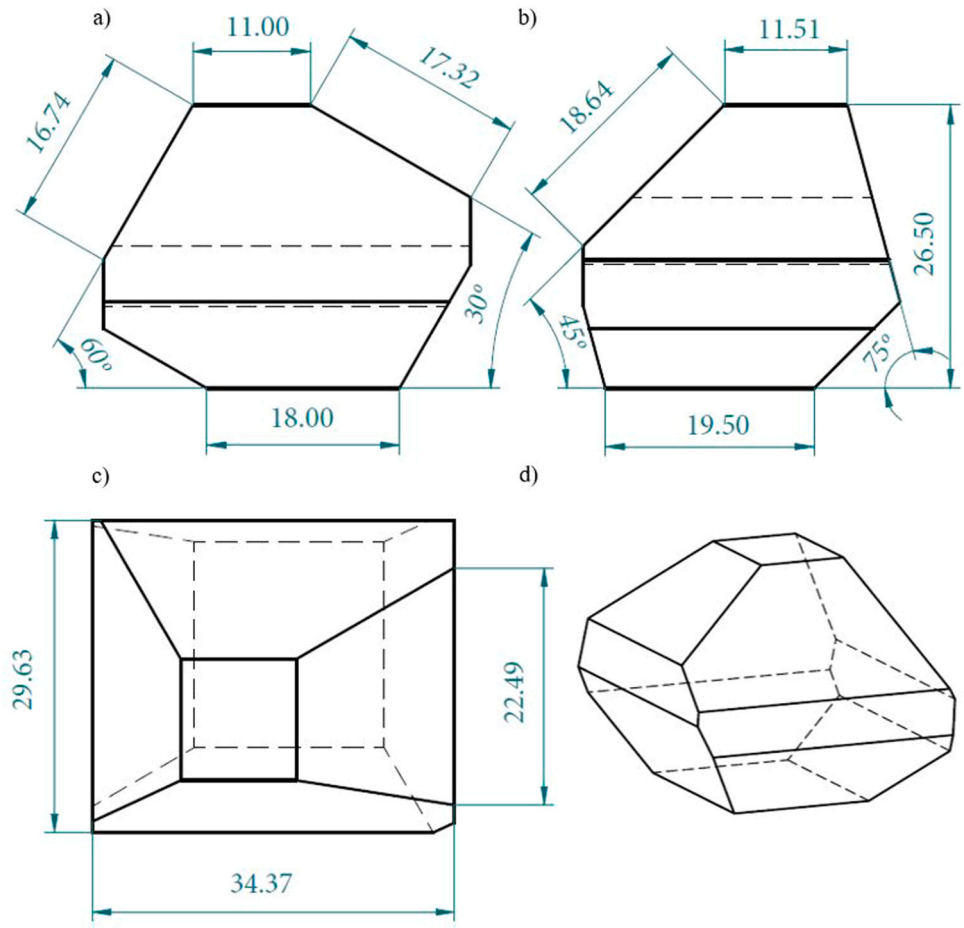

Fig. 5. Nominal dimensions (in mm) of four-faced part. Manufactured by SLS. a) Front. b) Left. c) Top. d) 3D view.

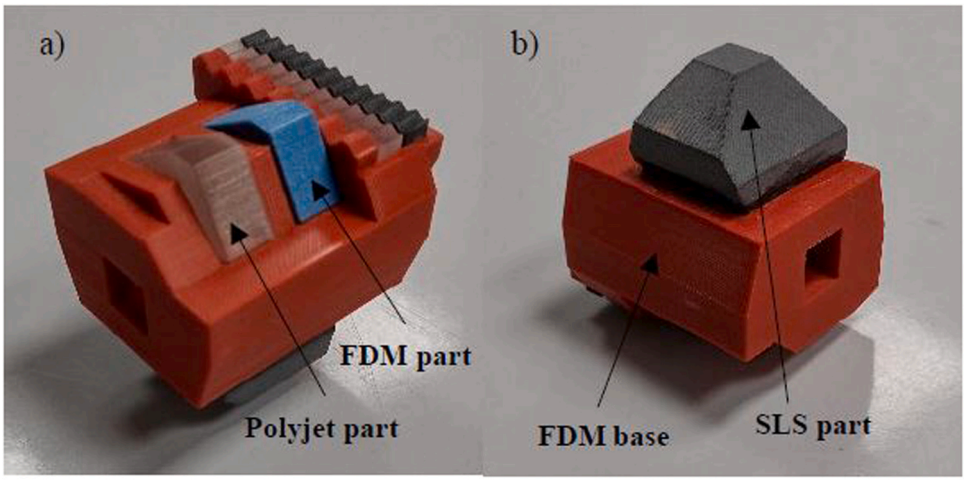

Fig. 6. Designed assembly. a) Upper view. b) Lower view.

evaluation.

4. Results and discussion

4.1. Surface filtering

Selection of the most suitable filtering cutoff for the surface evaluation have been made according to ISO 21920–3:2021 [35] for linear profile evaluation, and to UNE-EN ISO 25178–3 [33] for areal evaluation.

4.1.1. Linear filtering

Linear filtering, in roughness evaluation, is used to eliminate wave components present in primary profiles which does not belong to the roughness itself as defined in normative [35]. As roughness is within a band of wavelengths, two filters are applied: a long wavelength filter (λc) for low frequency waves, and short wavelength filter (λs), for high frequency waves.

Table 2
Range of geometries evaluated.

Technology	Material	Angle of inclination	Layer thickness/mm	Expected Ra/ μm
FDM	PLA	60° – 30°	0.2	25.00 – 43.30
FDM (base)	PLA	60° – 45° – 15°	0.1	12.50 – 17.67 – 24.14
Polyjet	Rigur RGD450	60° – 30°	0.1	12.50 – 21.65
SLS	PA12	60° – 45° – 30°	0.1	12.50 – 17.67 – 24.14

Table 3
XCT settings.

XCT settings	Value		
Voltage/kV	120	120	120
Current/μA	279	550	550
Physical filter	Al 2 mm	Al 2 mm	Al 2 mm
N° of projections	3000	1500	1500
Exposure time/ms	1000	500	500
Image averaging	No	Yes (2)	Yes (2)
Voxel size/μm	28	54	75

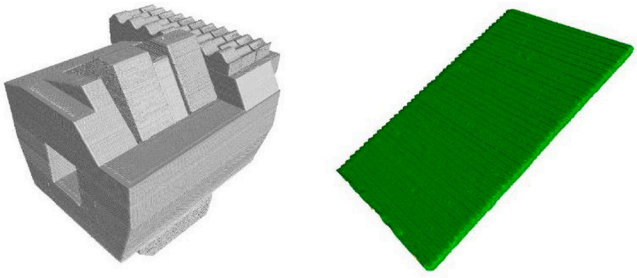

Fig. 7. XCT volume reconstruction – 28 μm voxel size (left) and example of ramp extracted in.STL (right).

According to Ra predicted values, λc cutoff should be 8 mm. ISO 21920 recommends a profile length of 40 mm (five times larger than sample length). As indicated in Section 3.2, maximum profile length is 15 mm. For the best adaptation possible to the dimensions and the normative, two different λc filter cutoff values were selected for profile evaluation:

- 8 mm λc cutoff is selected according to the Ra predicted value (for Ra values larger than 10 μm).
- 2.5 mm λc cutoff is selected according to the evaluation length. (12.5 mm, more similar to profile length).

An λs filter of 80 μm is selected according to the maximum resolution achievable for the voxel size obtained, as investigated in [40].

In Fig. 8 an example of profile distribution with its nominal length (12.5 mm) is displayed.

4.1.2. *Areal filtering*

Similar to linear roughness evaluation, a filtration is needed for the extraction of areal roughness parameters. For this purpose, 2D filters are applied: L-filter for low frequency waves and S-filter for high frequency waves.

Three 4 mm × 4 mm areas distributed across each ramp have been extracted, as displayed in the example in Fig. 9. L-filter nesting index (hi-pass filter) of 0.8 mm and an S-filter nesting index (low-pass filter) of 2.5 μm were selected.

4.2. *Theoretical and reference Ra comparison*

Results of preliminary experiment related to the geometries included in this study are shown in Table 4.

In general, most of measured Ra values have a deviation from theoretical values smaller than 5 μm, and no significant differences are found between both theoretical models for FDM results. As the study is focused on the performance of XCT, and thus, the deviation from results obtained by FVM measured reference values is the most important output, deviation from theoretical values is not in fact a critical parameter. However, it allows to have a first characterisation of the geometries, it is a good indicative of the correct performance of the manufacturing process (to ensure the viability of the study), and it makes it possible to consider theoretical values for analysis on next steps.

4.3. *Voxel size/Ra comparison*

First comparison is made taking into consideration the two key

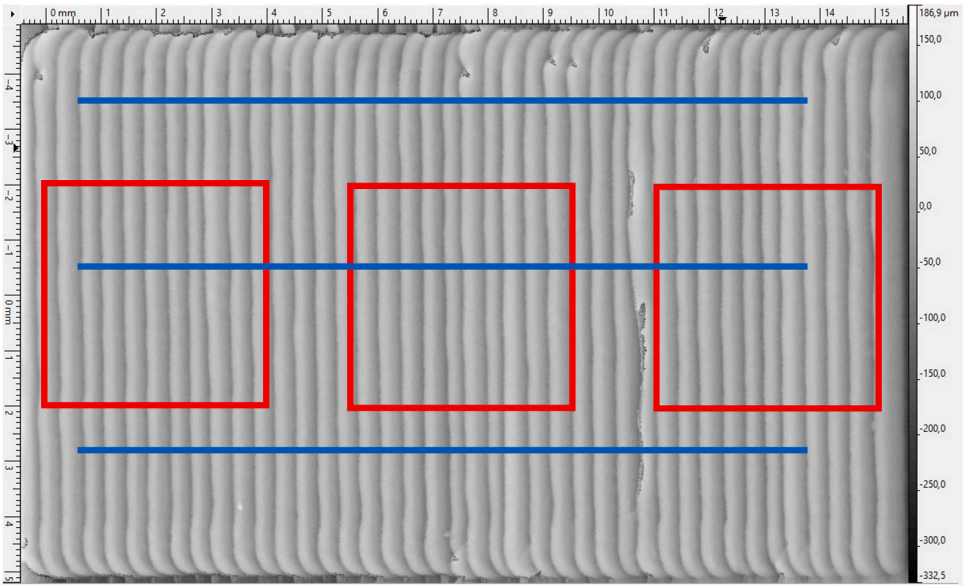

Fig. 8. Example of selected areas for surface evaluation. Linear profiles (blue), areas (red).

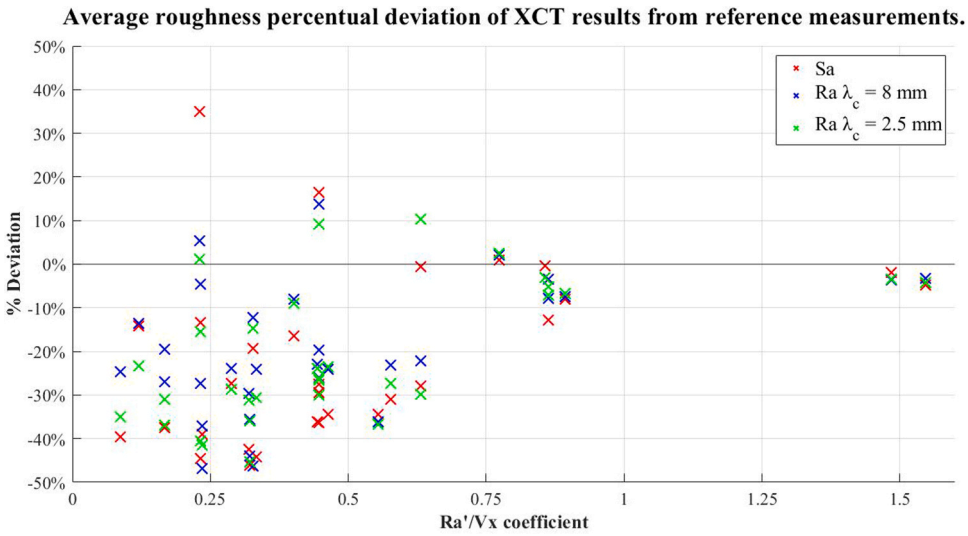

Fig. 9. Average roughness % deviation comparison.

Table 4
Comparison between theoretical and measured average roughness values.

Geometries	Ahn model theoretical Ra' [37]/μm	FDM optimised theoretical Ra'[38]/μm	FVM measured Ra/μm
Base – 15°	24.14	23.46	21.36
Base – 45°	17.67	17.98	17.60
Base – 60°	12.50	13.86	15.39
FDM – 30°	43.30	42.45	44.76
FDM – 60°	25.00	27.73	24.72
Polyjet – 30°	21.65	-	25.89
Polyjet – 60°	12.50	-	17.01
SLS – 30°	21.65	-	28.54
SLS – 45°	17.67	-	22.80
SLS – 60°	12.50	-	11.93

parameters: voxel size of XCT measurement (Vx) and theoretical average roughness (Ra'), calculated following predictive models [37,38] explained in Section 3.2.

A coefficient Ra'/Vx is settled for the comparisons. Fig. 9 summarizes the relationship between coefficient Ra'/Vx and the percentual deviation of XCT measurements from reference Alicona evaluation, in terms of average roughness (Ra and Sa).

Fig. 9 shows that the tendency of deviation values is in general negative, indicating that roughness values registered by XCT are mostly lower than roughness values registered by FVM; this happens due to the lower resolution of XCT devices comparing to FVM. A trend is identified for values of Ra'/Vx $\geq$ 0.75, where deviations are found to be progressively smaller and under 10% of the reference measurement. To validate the results, a measurement comparability evaluation using uncertainty calculations has been performed.

4.3.1. *Measurement comparability evaluation through uncertainty calculations*

For the validation of measurements, E_N parameter is calculated, according to normative ISO/IEC 17043:2023 [51], following the equation:

$$E_N = \frac{|y_{XCT} - y_{Alicona}|}{\sqrt{U_{XCT}^2 + U_{Alicona}^2}} \quad (4)$$

Where y_{XCT} = current measured value of the feature, $y_{Alicona}$ = calibrated value of the feature, U_{XCT} = expanded uncertainty of the XCT measurement and $U_{Alicona}$ = expanded uncertainty of calibration. Results are considered valid for $E_N \leq 1$ as stated in the normative.

Uncertainty calculations have been done following the procedures indicated in normative:

- ISO 15530–3:2011 [52] for reference Alicona measurements. Uncertainty results registered are in a range of $U_{Alicona}$ = 2–3 μm.
- VDI/VDE 2630–2.1 [53] for XCT measurements, also following the recommendations suggested in [5]. There is still not a standard for the determination of the uncertainties of XCT measurements, but this directive defines with good detail the factors to take into consideration, and it is commonly used [54,55]. Uncertainty results registered are in a range of U_{XCT} = 4–6 μm.

Values selected for the uncertainty calculations are Ra and Sa parameters, as used in the calculations for the percent deviation displayed in Fig. 9. In Fig. 10, the relationship of E_N parameter values with the coefficient Ra'/Vx, for each voxel size, is shown.

Distribution of values show that $E_N < 1$ complies for all measurements with Vx = 28 μm, which is not the case of measurements with Vx = 54 μm and Vx = 75 μm where most of values are over 1. It is shown also that the majority of the cases comply with the condition of $E_N < 1$ for a value of Ra'/Vx above 0,75; for the minimum voxel size achieved (28 μm), it will result in a theoretical limit value of Ra' = 21 μm.

No ramp Ra' value is over 0,75Vx for Vx = 75 μm, while the few cases for Vx = 54 μm do not fit into the $E_N < 1$ condition or are very close to 1. It is worth to mention that, even if it is true that $E_N < 1$, normative [51] recommends that if the value is very close to 1 (as it is the case of Vx = 54 μm results with Ra'/Vx above 0,75), validation should not be automatically done as desired value of E_N should be as close as possible to 0. Following this advice, it can be seen that none of Vx = 28 μm results with Ra'/Vx above 0,75 are close to 1. Therefore, with this calculations, it is possible to conclude that for this roughness values, tomographies with Vx = 54 μm and Vx = 75 μm are not suitable for roughness evaluation, and the most trustworthy results are those which coefficient Ra'/Vx $\geq$ 0.75.

4.3.2. *Voxel size and Ra' segmentation*

Additionally, a segmentation only by XCT voxel size is done according to Ra' = 21 μm value calculated as mentioned in Eq. 1, considering all technologies, divi. Results are displayed in Table 5, in terms of absolute and percentual deviation of the mean values.

Table 5 shows that only for Vx = 28 μm results are into the acceptable gap, especially for Ra' values > 21 μm where absolute differences

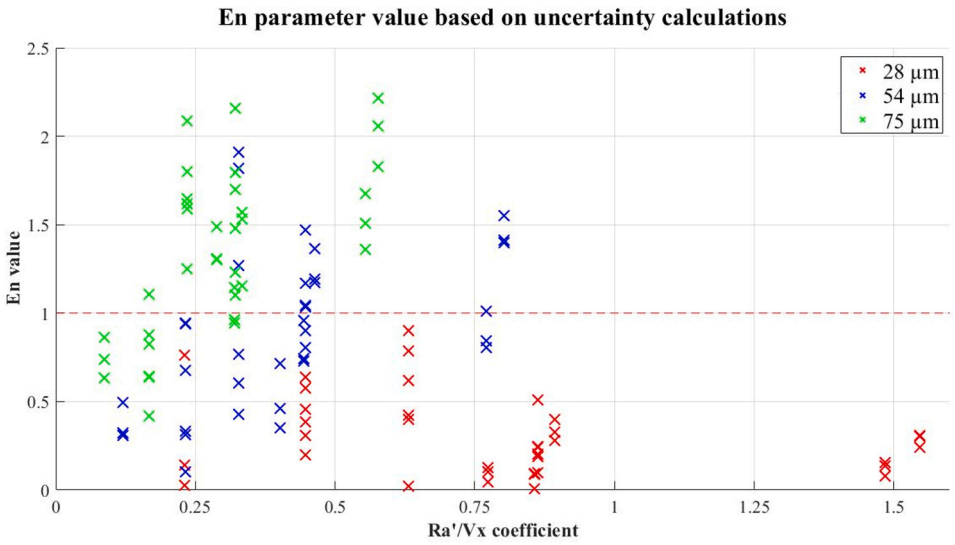

Fig. 10. En parameter comparison for each voxel size and Ra'/Vx coefficient.

Table 5
Absolute and percentual deviations of XCT results from reference measurements.

Ra/µm		*< 21*			*> 21*		
Voxel size/µm		*28*	*54*	*75*	*28*	*54*	*75*
Areal	Sa	-1.267	-5.897	-7.264	-0.637	-5.439	-8.559
	%	-9.83%	-45.75%	-56.35%	-2.85%	-24.37%	-38.35%
	Sq	-0.909	-6.571	-8.328	-0.343	-6.496	-10.116
	%	-5.86%	-42.36%	-53.69%	-1.30%	-24.61%	-38.33%
Linear λc = 8 mm	Ra	-2.077	-4.804	-5.332	-0.326	-4.71	-7.5
	%	-13.24%	-30.61%	-33.98%	-1.29%	-18.66%	-29.71%
	Rq	-2.447	-5.572	-6.344	-0.123	-5.428	-8.618
	%	-12.63%	-28.76%	-32.75%	-0.41%	-17.94%	-28.49%
Linear λc = 2.5 mm	Ra	-2.755	-6.129	-6.502	-0.568	-5.065	-8.319
	%	-19.78%	-44.02%	-46.70%	-2.32%	-20.73%	-34.05%
	Rq	-2.853	-6.75	-7.482	-0.474	-5.935	-9.744
	%	-16.72%	-39.57%	-43.86%	-1.63%	-20.47%	-33.61%

are below 1 µm. This also confirms the results obtained in Section 4.3.1. In general terms, it is shown that Sa and Sq values are more similar to Ra and Rq values with a λc = 2.5 mm cutoff than with a λc = 8 mm cutoff; however, for Ra' values < 21 µm and Vx = 28 µm higher differences are found. Thus, the influence of the AM technology has been investigated.

4.4. AM technology comparison

Focusing in Vx= 28 µm XCT measurements, segmentation into AM technologies is presented in Fig. 11.

Ra and Rq parameters are similar in both FDM and Polyjet features,

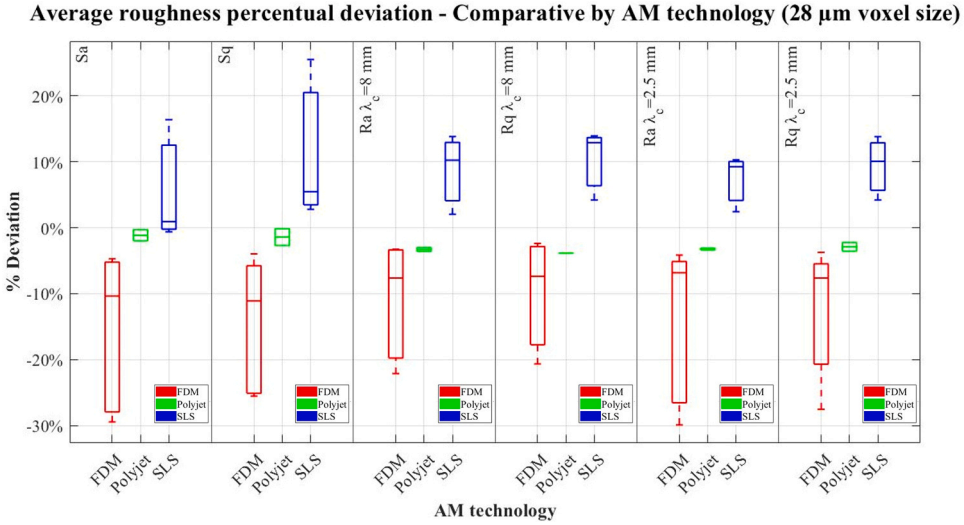

Fig. 11. Average roughness % deviation comparison - AM Technology segmentation.

with a higher negative % difference in FDM mean values due to higher volume of surfaces with Ra'< 21 μm in the sample. However, higher variances are displayed in Sa and Sq values for SLS geometries; also, differences are positive, indicating that average roughness values registered are higher than in reference measurements.

The reason for the variance in Sa-Ra and Sq-Rq results is the non-uniform surface. Unlike FDM and Polyjet processes, the presence of randomly distributed unfused dust in the surface creates unequal profiles in both X and Y directions. Although post process is done to remove the unfused dust, an amount of this remains in the surface because, as explained in Section 3.2, it is not possible to remove all the powder without damaging the surface. In FDM and Polyjet surfaces, roughness profiles are present predominantly in the perpendicular direction to the layer stairs. This dimension added to surface measurements increases the error in areal measurements.

A graphical view of an example of the reconstructed surfaces in each AM technology can be seen in Fig. 12. The higher Ra values can be explained also due to the unfused surface powder (Fig. 13). Its presence, added to the characteristics of AM technologies, could create re-entry features which cannot be evaluated by optical microscopes, because they are out of the field of view. However, XCT devices can perform measurements of internal and non-accessible elements, being able to characterize re-entries and, thus, increasing the average roughness parameters' values.

4.5. Skewness and kurtosis

Skewness and kurtosis determine the shape of the profile/area extracted. Higher values of skewness parameters (Ssk, Rsk) are indicatives of a predominancy of sharp peaks, while lower values indicate a higher number of rifts. On the other hand, the lower are the kurtosis values (Sku, Rku), the smoother are the peaks and valleys.

Both skewness and kurtosis values have been evaluated. The mean value of the differences from the reference measurements are registered and shown in Fig. 14 for skewness and kurtosis parameters. As in the previous section, results are focused on Vx= 28 μm XCT measurements.

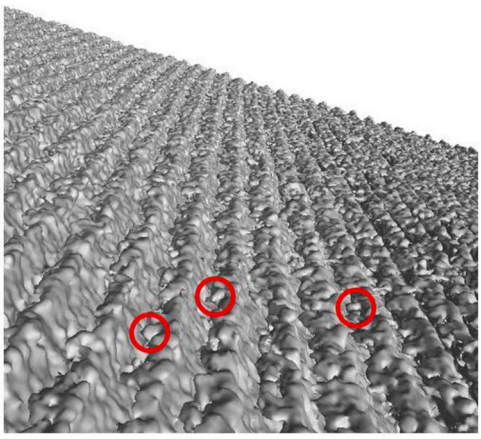

Fig. 13. Close up of an SLS surface in XCT, showing the unfused powder representation (examples circled in red).

Results show that deviations from references are considerably low for FDM and Polyjet technologies, indicating a slightly higher skewness and kurtosis. For SLS technology, results show greater differences, presenting lower skewness and higher kurtosis.

XCT measurements, because their capacity of measuring elements out of direct sight, are able to produce sharper surfaces in spite of the lower resolution (Fig. 15). It becomes clearer for SLS surfaces, where re-entries caused by unfused powder are more present, and thus differences are higher. It also produces a negative difference in skewness because some deep valleys are not accessible for optical measurements.

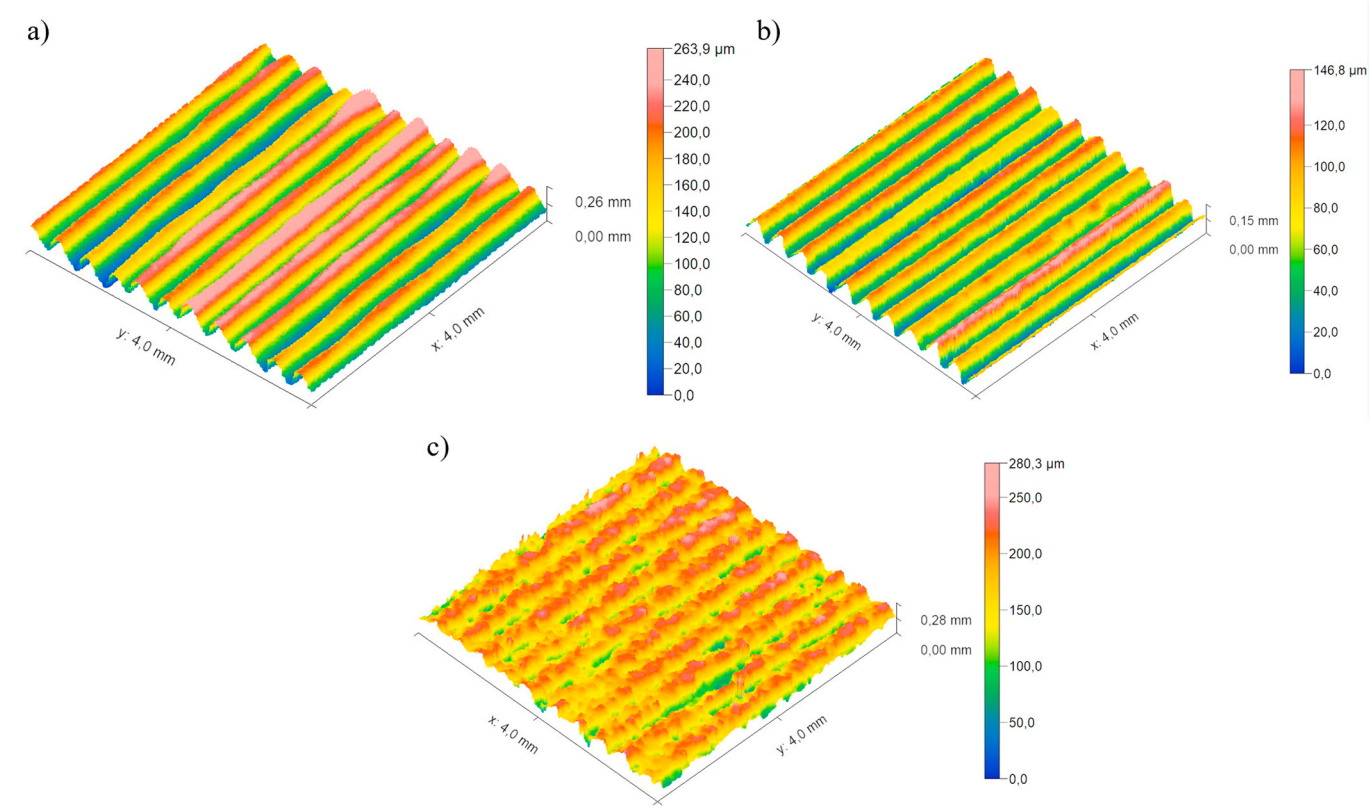

Fig. 12. Surface height colour maps obtained from XCT reconstructions. a) FDM, b) Polyjet, c) SLS.

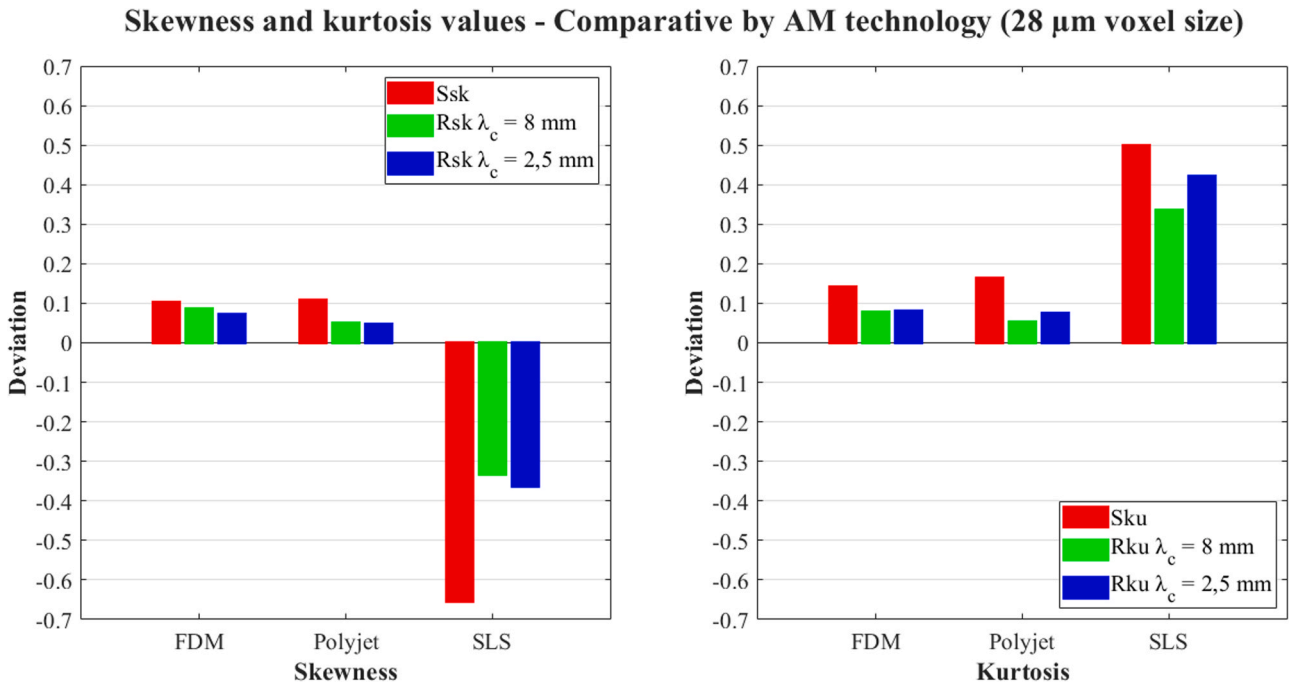

Fig. 14. Skewness and kurtosis deviations from references.

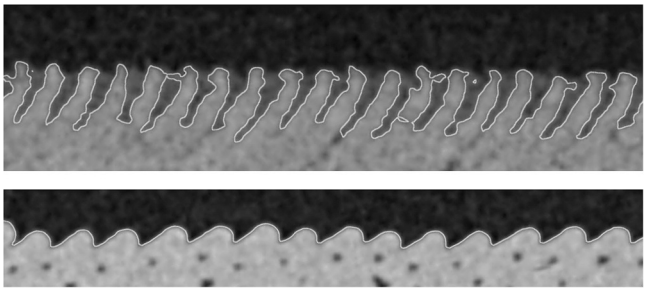

Fig. 15. Profile comparison of profiles in XCT. SLS (upper) and FDM (lower).

4.6. *Maximum roughness*

The roughness values of highest peaks (Sp, Rp) and deeper valleys (Sv, Rv), apart from maximum roughness value (Sz, Rz) is studied. Percent deviations of areal (Fig. 16) and linear (Fig. 17) are presented. As mentioned before, results are focused on Vx= 28 µm XCT measurements.

Results show an equilibrium between peaks and valleys in Polyjet results, with a slight negative deviation. FDM surfaces presents higher deviations, with an emphasis on valleys; as resolution is lower than optical measurements, deep valleys tend to be smoothed and maximum values are lower. Opposite happens on SLS surfaces because, as mentioned before, re-entries and out-of-sight elements are not reached by optical FVM. Also, linear measurements show a different tendency than areal parameters due to the non-uniform stairs, as commented in Section 4.4.

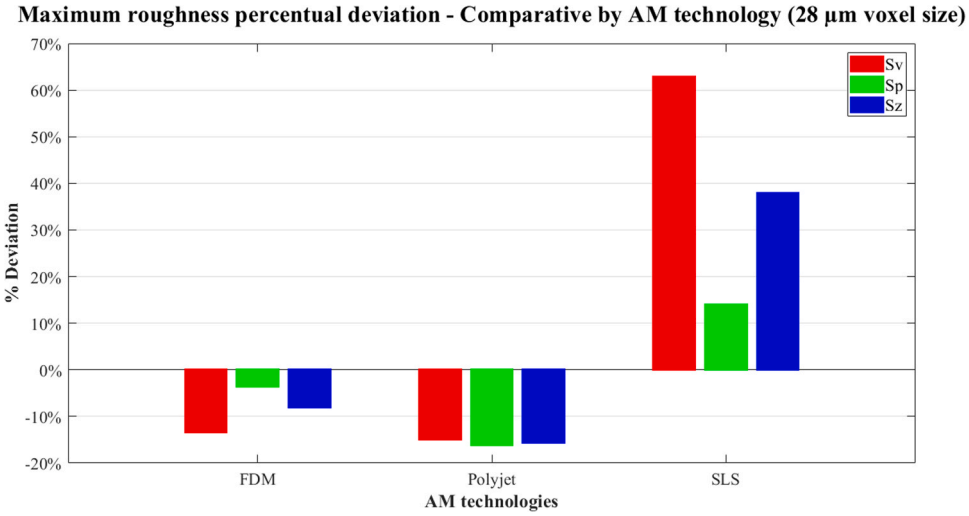

Fig. 16. Areal roughness maximum values % deviation.

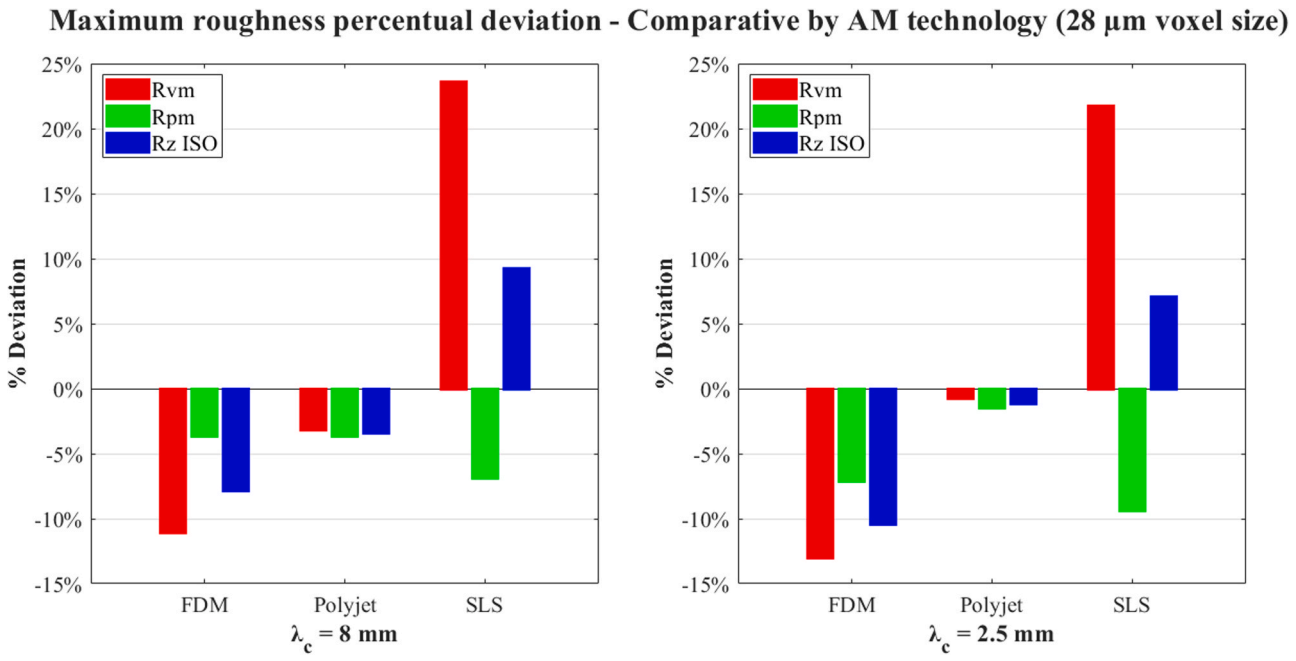

Fig. 17. Linear roughness maximum values % deviation for λc = 8 mm (left) and λc = 2,5 mm (right).

5. Discussion

First analysis of the results shows that, as expected, deviations of the XCT measurements and reference FVM measurements follow a tendency in which smaller XCT voxel size is correlated with better accuracy. A value of Ra'/Vx ≈ 0.75 is found to be a limit where, for higher values, it is possible to characterise surface texture for this type of polymeric AM parts with an acceptable precision. However, it is also found that small geometrical magnifications and, thus, high voxel sizes, remain non useful as deviations increase. In this experiment, Vx = 28 µm has been found suitable, which is an achievable geometrical magnification by a commercial XCT device for industrial parts with common dimensions. Analysis have been focused on this geometrical magnification from this segmentation, and validation by an uncertainty calculation [52,53] and measurement compatibility analysis [51] have been done.

Regarding the three polymeric AM technologies studied, post-processing has been seen as an important factor in the characterisation of the surfaces. No abrasive method has been applied with the objective of reducing the possible damage originated; as stated in Section 3.2, pressurized water is the recommended method by the manufacturer, and the pressure was controlled by the cleaning device. Support material sticked to the surface is weak enough to be removed by the water, not eroding the steps. Regarding SLS, compressed air was not filled with abrasive particles not to damage the surface; the main disadvantage is that the cleaning capacity of compressed air has been demonstrated not to be enough to remove all the powder. While theoretical values were achieved more precisely for FDM, which has no post process, therefore no surface modification (seen in the preliminary study), it has been found that it affects in a different way in terms of XCT accuracy comparing to optical devices (FVM in this case).

Polyjet surfaces, which are post processed by pressurized water, show same level of accuracy or even higher when characterised by XCT than FDM surfaces which has no post process. On the other hand, SLS parts, post processed by compressed air, have higher deviations and less predictable results. The reasons of this SLS surface behaviour are mainly unfused powder and re-entry geometries. Both aspects are linked because unfused powder create small voids out of the general stair-stepped shape of the surface. This unpredictable features can be reached by XCT but are out of sight of optical measuring devices, causing sharper surfaces with deeper valleys and higher roughness values.

In FDM and Polyjet features, unlike SLS, surfaces obtained by XCT are in general smoother than by FVM mainly because the lower resolution of the XCT devices, as expected. Increasing the voxel size and, thus, reducing the resolution, leads to less detailed surface data. This XCT smoothing effect is also present in SLS but is seen to be weaker than the effect of re-entrant features created by the unfused powder.

Additionally, roughness evaluation by linear and areal parameters shows no significant difference in FDM and Polyjet parts, while areal parameters have a better agreement between XCT and reference evaluation methods than linear ones for SLS parts. As seen in Fig. 13, linear profiles can be extracted in the perpendicular direction to the AM layers with no big shape variation in FDM and Polyjet ramps, therefore those profiles are more similar along the feature. Consequently, results are more likeable to be repeated along the surface, and thus more similar to the complete area evaluation. In SLS, again, unfused powder creates more heterogeneous profiles with different values. This is why an evaluation by areal parameters is demonstrated to be more suitable for the whole SLS surface.

Finally, regarding λs filter selected, value recommended by normative for the corresponding λc filter is 8 µm for the 2.5 mm λc cutoff, and 25 µm for the 8 mm λc cutoff. However, as investigated in [40], a λs filter of 80 µm (best resolution achievable for a voxel size around 20–30 µm) creates no difference in Ra measurements, because dominant surface texture components have a spatial wavelength larger than 80 µm. It becomes clearer for higher voxel size (54 µm and 75 µm), in which resolution is lower and, thus, wavelength of texture components is bigger.

6. Conclusions and future work

In this paper, a metrological characterisation of polymeric additive manufactured surfaces by XCT for the evaluation of the performance of the metrological technique is presented. Different additive manufacturing technologies and parameters as angle of inclination and layer thickness are used to create inclined ramps, with a range of theoretical average roughness (Ra) according to predictive models [37,38].

A preliminary study was made with the objective of a first feature

characterisation, and as a result it has been a selection for this final experiment of only the most precise geometries according to the trueness of FVM measurements comparing to the theoretical predictions. This segmentation is made due to the objective of creating a compact object of study, improving this way the geometrical magnification of the XCT measurement; also, the dimensions should be similar to a common industrial part. Selected features are distributed along an ad hoc designed assembly, optimised for its evaluation both in an XCT machine, and in a reference device (FVM). Roughness areal and linear parameters are extracted, and a comparison has been made for a XCT performance evaluation.

Results show a tendency in the relationship between voxel size (Vx) and predicted average roughness (Ra'), in which a value of Ra'/Vx ≈ 0.75 is found to be a starting point for accurate XCT roughness measurements. Results have been validated by an uncertainty calculation following normative [52,53], with a measurement compatibility analysis [51] However, as previously studied, resolution remains as a handicap for XCT measurements regarding surface evaluation, but it is demonstrated that for a reasonably achievable geometrical magnification for a part with industrial dimensions (28 μm voxel size for a 50 mm × 55 mm × 60 mm part, in this case), it is possible to evaluate roughness with an acceptable precision.

Characterisation of 3 different polymeric AM technologies have been made, and therefore their topographical behaviour was possible to evaluate. Post process was found to be an important parameter to consider, working in a different way for Polyjet (where post processing affects the trueness of the FVM results, but has little effect in XCT comparison) and for SLS (where unfused powder and re-entrant features creates different topography and roughness results between XCT and optical measurements). Although post process has been necessary for a correct cleaning of the parts, as expected, it has found not to be completely perfect and non-automated as material remain unevenly in the surface in both technologies.

Linear and areal roughness parameters calculation have led to the conclusion that both FDM and Polyjet surfaces are suitable to be evaluated with linear profiles perpendicular to the steps created by the layer-by-layer technology. On the other hand, SLS surfaces need an areal characterisation for more accurate results, again, because the unfused powder creates more heterogeneous profiles with high roughness differences between them.

To conclude, in this study a surface characterisation of a wide range of polymeric AM surfaces, made of different AM technologies with different AM principles (fused filament, Polyjet, powder sintering), considering dimensional parameters and optimising the object of study to be suitable for both XCT and optical reference devices has been made. However, as in a single study is difficult to evaluate every individual case, further research should be done to achieve a fully generalised characterisation of this type of parts. For this future work, including non-planar geometries could be interesting to check the effect of form in surface roughness. Micro XCT could be used also for a more precise evaluation; however, geometrical magnification could still be a disadvantage depending on the size of the part.

CRediT authorship contribution statement

Díaz-Pérez Lucía Candela: Writing – review & editing, Supervision, Resources, Conceptualization. **Gallardo Artal Daniel:** Writing – original draft, Visualization, Validation, Methodology, Investigation, Formal analysis, Conceptualization. **Torralba Marta:** Writing – review & editing. **Jiménez Roberto:** Writing – review & editing. **Albajez José Antonio:** Writing – review & editing, Supervision, Resources, Project administration, Funding acquisition, Conceptualization. **Yagüe-Fabra José Antonio:** Writing – review & editing, Supervision, Project administration, Funding acquisition.

Declaration of Competing Interest

The authors declare that they have no known competing financial interests or personal relationships that could have appeared to influence the work reported in this paper.

Data Availability

Data will be made available on request.

Acknowledgements

This work was supported by project RTI2018–097191-B-I00 funded by MCIN/AEI/ 10.13039/501100011033 and by ERDF A way of making Europe; by project PID2021–127134 O-B-I00 funded by MCIN/AEI/ 10.13039/501100011033 and by ERDF A way of making Europe; and by grant PRE2019–089465 funded by MCIN/AEI/ 10.13039/501100011033 and by ESF Investing in your future.

References

[1] M. Ferrucci, R.K. Leach, C. Giusca, S. Carmignato, W. Dewulf, Towards geometrical calibration of x-ray computed tomography systems - a review, Meas. Sci. Technol. 26 (2015), https://doi.org/10.1088/0957-0233/26/9/092003.
[2] A. Cantatore, P. Müller, Introduction to computed tomography, 2011.
[3] G. Moroni, S. Petrò, Design for X-ray computed tomography, Procedia CIRP 84 (2019) 173–178, https://doi.org/10.1016/j.procir.2019.04.342.
[4] W. Sun, S. Brown, R. Leach, An overview of industrial X-ray computed tomography, 2012.
[5] H. Villarraga-Gómez, C.B. Lee, S.T. Smith, Dimensional metrology with X-ray CT: a comparison with CMM measurements on internal features and compliant structures, Precis Eng. 51 (2018) 291–307, https://doi.org/10.1016/j.precisioneng.2017.08.021.
[6] H. Villarraga-Gómez, E.L. Herazo, S.T. Smith, X-ray computed tomography: from medical imaging to dimensional metrology, Precis Eng. 60 (2019) 544–569, https://doi.org/10.1016/j.precisioneng.2019.06.007.
[7] M. Yang, X.L. Wang, Y.P. Liu, F.Y. Meng, X.D. Li, W.L. Liu, D.B. Wei, Automatic calibration method of voxel size for cone-beam 3D-CT scanning system, Chin. Phys. C. 38 (2014), https://doi.org/10.1088/1674-1137/38/4/046202.
[8] A.-F. Obaton, C. Gottlieb Klingaa, C. Rivet, K. Mohaghegh, S. Baier, J. Lasson Andreasen, L. Carli, L. de Chiffre, Reference standards for XCT measurements of additively manufactured parts, 10th Conf. Ind. Comput. Tomogr. (ICT), Wels, Austria (2020) www.ict-conference.com/2020.
[9] P. Hermanek, F. Borges De Oliveira, S. Carmignato, M. Bartscher, Experimental investigation of new multi-material gap reference standard for testing computed tomography systems, 7th Conf. Ind. Comput. Tomogr. (ICT), Leuven, Belg. (2017).
[10] C.M. Shakarji, V. Srinivasan, V.D. Lee, M. Shilling, B. Muralikrishnan, Standards for Evaluating the Influence of Materials on the Performance of X-ray Computed Tomography in Measuring Geometric Variability, Int. Mech. Eng. Congr. Expo. (IMECE), Portland, USA (2020).
[11] R.H. Schmitt, A. Buratti, N. Grozmani, C. Voigtmann, M. Peterek, Model-based optimisation of CT imaging parameters for dimensional measurements on multimaterial workpieces, CIRP Ann. 67 (2018) 527–530, https://doi.org/10.1016/j.cirp.2018.04.003.
[12] H. Villarraga-Gómez, A. Amirkhanov, C. Heinzl, S.T. Smith, Assessing the effect of sample orientation on dimensional X-ray computed tomography through experimental and simulated data, Meas. (Lond.) 178 (2021), https://doi.org/10.1016/j.measurement.2021.109343.
[13] J.J. Lifton, S. Carmignato, Simulating the influence of scatter and beam hardening in dimensional computed tomography, Meas. Sci. Technol. 28 (2017), https://doi.org/10.1088/1361-6501/aa80b2.
[14] M. Reiter, F.B. de Oliveira, M. Bartscher, C. Gusenbauer, J. Kastner, Case study of empirical beam hardening correction methods for dimensional x-ray computed tomography using a dedicated multi-material reference standard, J. Nondestr Eval. 38 (2019), https://doi.org/10.1007/s10921-018-0548-3.
[15] J.J. Lifton, A.A. Malcolm, Estimating the product of the x-ray spectrum and quantum detection efficiency of a ct system and its application to beam hardening correction, Sensors 21 (2021), https://doi.org/10.3390/s21093284.
[16] E. Morse, Design for Metrology – A new idea? Procedia CIRP 84 (2019) 165–168, https://doi.org/10.1016/j.procir.2019.04.240.
[17] M.A. de Pastre, S.C. Toguem Tagne, N. Anwer, Test artefacts for additive manufacturing: a design methodology review, CIRP J. Manuf. Sci. Technol. 31 (2020) 14–24, https://doi.org/10.1016/j.cirpj.2020.09.008.
[18] A. Wiberg, J. Persson, J. Ölvander, Design for additive manufacturing – a review of available design methods and software, Rapid Prototyp. J. 25 (2019) 1080–1094, https://doi.org/10.1108/RPJ-10-2018-0262.
[19] H. Bikas, A.K. Lianos, P. Stavropoulos, A design framework for additive manufacturing, Int. J. Adv. Manuf. Technol. 103 (2019) 3769–3783, https://doi.org/10.1007/s00170-019-03627-z.

[20] V.M. Rivas Santos, A. Thompson, D. Sims-Waterhouse, I. Maskery, P. Woolliams, R. Leach, Design and characterisation of an additive manufacturing benchmarking artefact following a design-for-metrology approach, Addit. Manuf. 32 (2020), https://doi.org/10.1016/j.addma.2019.100964.
[21] G.A.O. Adam, D. Zimmer, Design for Additive Manufacturing-Element transitions and aggregated structures, CIRP J. Manuf. Sci. Technol. 7 (2014) 20–28, https://doi.org/10.1016/j.cirpj.2013.10.001.
[22] R. Leach, S. Carmignato, Precision Metal Additive Manufacturing, 2021.
[23] S. Singh, S. Ramakrishna, R. Singh, Material issues in additive manufacturing: a review, J. Manuf. Process 25 (2017) 185–200, https://doi.org/10.1016/j.jmapro.2016.11.006.
[24] K. Lussenburg, A. Sakes, P. Breedveld, Design of non-assembly mechanisms: a state-of-the-art review, Addit. Manuf. 39 (2021), https://doi.org/10.1016/j.addma.2021.101846.
[25] Y. Chahid, R. Racasan, L. Pagani, A. Townsend, A. Liu, P. Bills, L. Blunt, Parametrically designed surface topography on CAD models of additively manufactured lattice structures for improved design validation, Addit. Manuf. 37 (2021), https://doi.org/10.1016/j.addma.2020.101731.
[26] G.A.O. Adam, D. Zimmer, On design for additive manufacturing: evaluating geometrical limitations, Rapid Prototyp. J. 21 (2015) 662–670, https://doi.org/10.1108/RPJ-06-2013-0060.
[27] R.K. Leach, D. Bourell, S. Carmignato, A. Donmez, N. Senin, W. Dewulf, Geometrical metrology for metal additive manufacturing, CIRP Ann. 68 (2019) 677–700, https://doi.org/10.1016/j.cirp.2019.05.004.
[28] W. Sun, D.R. Symes, C.M. Brenner, M. Böhnel, S. Brown, M.N. Mavrogordato, I. Sinclair, M. Salamon, Review of high energy X-ray computed tomography for non-destructive dimensional metrology of large metallic advanced manufactured components, Rep. Prog. Phys. 85 (2022), https://doi.org/10.1088/1361-6633/ac43f6.
[29] T. Hofstätter, D.B. Pedersen, G. Tosello, H.N. Hansen, Applications of Fiber-Reinforced Polymers in Additive Manufacturing, Procedia CIRP 66 (2017) 312–316, https://doi.org/10.1016/j.procir.2017.03.171.
[30] A. García-Collado, J.M. Blanco, M.K. Gupta, R. Dorado-Vicente, Advances in polymers based multi-material additive-manufacturing techniques: state-of-art review on properties and applications, Addit. Manuf. 50 (2022), https://doi.org/10.1016/j.addma.2021.102577.
[31] Geometric product specifications (GPS). surface texture: profile method: rules and procedures for the assessment of surface texture (ISO 4288:1996), British Standards Institution, 1998.
[32] Geometrical product specifications (GPS). Surface texture: Areal. Part 2: Terms, definitions and surface texture parameters (ISO 25178–2:2011), 2011.
[33] Geometrical product specifications (GPS). Surface texture: Areal. Part 3: Specification operators (ISO 25178–3:2012)., 2012.
[34] Geometrical product specifications (GPS). Surface texture: Areal. Part 6: Classification of methods for measuring surface texture (ISO 25178–6:2010), 2010.
[35] Geometrical product specifications (GPS). Surface texture: Profile. Part 3: Specification operators (ISO 21920–3:2021), 2021. www.iso.org.
[36] M.E. Imanian, F.R. Biglari, Modeling and prediction of surface roughness and dimensional accuracy in SLS 3D printing of PVA/CB composite using the central composite design, J. Manuf. Process 75 (2022) 154–169, https://doi.org/10.1016/j.jmapro.2021.12.065.
[37] I. Dzullijah, D. Songlin, S. Shoujin, Roughness Prediction For FDM Produced Surfaces, Int. Inst. Eng. (2014), https://doi.org/10.15242/iie.e0214527.
[38] I. Buj-Corral, A. Domínguez-Fernández, R. Durán-Llucià, Influence of Print Orientation on Surface Roughness in Fused Deposition Modeling (FDM) Processes, Materials 12 (2019) 3834, https://doi.org/10.3390/ma12233834.
[39] H. Villarraga-Gómez, E.P. Morse, S.T. Smith, Assessing the effect of penetration length variations on dimensional measurements with X-ray computed tomography, Precis Eng. 79 (2023) 146–163, https://doi.org/10.1016/j.precisioneng.2022.10.001.
[40] W. Sun, C. Giusca, S. Lou, X. Yang, X. Chen, T. Fry, X. Jiang, A. Wilson, S. Brown, H. Boulter, Establishment of X-ray computed tomography traceability for additively manufactured surface texture evaluation, Addit. Manuf. 50 (2022), https://doi.org/10.1016/j.addma.2021.102558.
[41] B. He, H. Zheng, S. Ding, R. Yang, Z. Shi, A review of digital filtering in evaluation of surface roughness, Metrol. Meas. Syst. 28 (2021) 217–253, https://doi.org/10.24425/mms.2021.136606.
[42] A. Townsend, R. Racasan, P. Bills, L. Blunt, Development of an interlaboratory comparison investigating the generation of areal surface texture data per ISO 25178 from XCT, in: 7th Conference on Industrial Computed Tomography (ICT), Leuven, Belgium, 2017. www.iCT2017.org.
[43] N. Ortega, S. Plaza, A. Pascual, I. Holgado, L.N. López De Lacalle, Study of the influence of filter material on the roughness evaluation by means of CT, in: Euspen's 20th International Conference and Exhibition, Geneva, CH, 2020.
[44] A. Townsend, L. Pagani, P. Scott, L. Blunt, Areal surface texture data extraction from X-ray computed tomography reconstructions of metal additively manufactured parts, Precis Eng. 48 (2017) 254–264, https://doi.org/10.1016/j.precisioneng.2016.12.008.
[45] L. Pagani, A. Townsend, W. Zeng, S. Lou, L. Blunt, X.Q. Jiang, P.J. Scott, Towards a new definition of areal surface texture parameters on freeform surface: re-entrant features and functional parameters, Meas. (Lond.) 141 (2019) 442–459, https://doi.org/10.1016/j.measurement.2019.04.027.
[46] S. Carmignato, V. Aloisi, F. Medeossi, F. Zanini, E. Savio, Influence of surface roughness on computed tomography dimensional measurements, CIRP Ann. Manuf. Technol. 66 (2017) 499–502, https://doi.org/10.1016/j.cirp.2017.04.067.
[47] S. Petzold, J. Klett, T.A. Osswald, A. Statistical, Study of surface roughness for polyamide 12 parts produced using selective laser sintering, international polymer processing, J. Polym. Process. Soc. 35 (2020) 126–138.
[48] N.K. Maurya, V. Rastogi, P. Singh, Comparative study and measurement of form errors for the component printed by FDM and polyjet process, Instrum. Mes. Metrol. 18 (2019) 353–359, https://doi.org/10.18280/i2m.180404.
[49] C. Sen, G. Dursun, A. Orhangul, G. Akbulut, Assessment of additive manufacturing surfaces using x-ray computed tomography, in: Procedia CIRP, Elsevier B.V., 2022, pp. 501–506, https://doi.org/10.1016/j.procir.2022.03.078.
[50] A. Townsend, L. Pagani, L. Blunt, P.J. Scott, X. Jiang, Factors affecting the accuracy of areal surface texture data extraction from X-ray CT, CIRP Ann. Manuf. Technol. 66 (2017) 547–550, https://doi.org/10.1016/j.cirp.2017.04.074.
[51] Conformity assessment. General requirements for the competence of proficiency testing providers (ISO/IEC 17043:2023), 2023.
[52] Geometrical product specifications (GPS). Coordinate measuring machines (CMM). Technique for determining the uncertainty of measurement. Part 3: Use of calibrated workpieces or measurement standards. (ISO 15530–3:2011), 2011.
[53] Computed tomography in dimensional measurement. VDI/VDE 2630 Part 2.1: Determination of the uncertainty of measurement and the test process suitability of coordinate measurement systems with CT sensors, 2015.
[54] Á. Rodríguez-Sánchez, A. Thompson, L. Körner, N. Brierley, R. Leach, Review of the influence of noise in X-ray computed tomography measurement uncertainty, Precis Eng. 66 (2020) 382–391, https://doi.org/10.1016/j.precisioneng.2020.08.004.
[55] M. Praniewicz, J.C. Fox, C. Saldana, Toward traceable XCT measurement of AM lattice structures: uncertainty in calibrated reference object measurement, Precis Eng. 77 (2022) 194–204, https://doi.org/10.1016/j.precisioneng.2022.05.010.